AD-A039 636 NAVAL RESEARCH LAB WASHINGTON D C F/G 17/7
PERFORMANCE LIMITS OF A DUAL-ACOUSTIC-CHANNEL SURFACE-ACOUSTIC---ETC(U)
APR 77 M FINNLEY, C BANKS, D C WEBB
UNCLASSIFIED NRL-8116 NL

| OF |
AD
A039636

END
DATE
FILMED
6-77

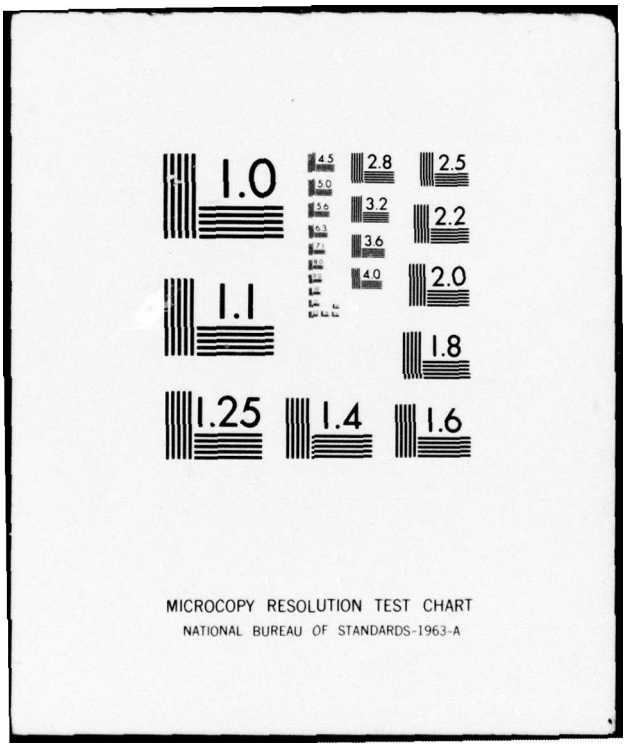
1.0
1.1
1.25
1.4
1.6
1.8
2.0
2.2
2.5
2.8
3.2
3.6
4.0
4.5
5.0
5.6
6.3
7.1
MICROCOPY RESOLUTION TEST CHART
NATIONAL BUREAU OF STANDARDS-1963-A

NRL Report 8116

Performance Limits of a Dual-Acoustic-Channel Surface-Acoustic-Wave (SAW) Interferometer

M. FINNLEY, C. BANKS, AND D. C. WEBB
Microwave Techniques Branch
Electronics Technology Division

12

April 19, 1977

NAVAL RESEARCH LABORATORY
Washington, D.C.

SECURITY CLASSIFICATION OF THIS PAGE *(When Data Entered)*

REPORT DOCUMENTATION PAGE

READ INSTRUCTIONS BEFORE COMPLETING FORM

1. REPORT NUMBER: NRL Report 8116
2. GOVT ACCESSION NO.:
3. RECIPIENT'S CATALOG NUMBER:

4. TITLE *(and Subtitle)*: PERFORMANCE LIMITS OF A DUAL-ACOUSTIC-CHANNEL SURFACE-ACOUSTIC-WAVE (SAW) INTERFEROMETER

5. TYPE OF REPORT & PERIOD COVERED: Final report on one phase of a continuing NRL problem

6. PERFORMING ORG. REPORT NUMBER:

7. AUTHOR(s): M. Finnley, C. Banks and D.C. Webb

8. CONTRACT OR GRANT NUMBER(s):

9. PERFORMING ORGANIZATION NAME AND ADDRESS: Naval Research Laboratory, Washington, D.C. 20375

10. PROGRAM ELEMENT, PROJECT, TASK AREA & WORK UNIT NUMBERS: NRL Problem R08-54, Project RR021-03-46

11. CONTROLLING OFFICE NAME AND ADDRESS: Department of the Navy, Office of Naval Research, Arlington, Va. 22217

12. REPORT DATE: April 19, 1977

13. NUMBER OF PAGES: 22

14. MONITORING AGENCY NAME & ADDRESS *(if different from Controlling Office)*

15. SECURITY CLASS. *(of this report)*: Unclassified

15a. DECLASSIFICATION/DOWNGRADING SCHEDULE

16. DISTRIBUTION STATEMENT *(of this Report)*

Approved for public release; distribution unlimited

17. DISTRIBUTION STATEMENT *(of the abstract entered in Block 20, if different from Report)*

18. SUPPLEMENTARY NOTES

19. KEY WORDS *(Continue on reverse side if necessary and identify by block number)*

Surface acoustic waves
Interferometers
Navigation satellites
NAVSTAR Global Positioning System

20. ABSTRACT *(Continue on reverse side if necessary and identify by block number)*

Design, construction, and performance of a dual-acoustic-channel interferometer, capable of placing nulls spaced every 150 kHz from 329.15 to 335 MHz, is described. The prototype device constructed exhibited a minimum null depth for 40 consecutive nulls of 33 dB, with more than half the nulls being 45 dB or more. Midband insertion loss was 27 dB. Second-order effects, such as spurious signals, required some design tradeoffs. Slight modifications of the prototype should enable 50 dB nulls to be achieved with an insertion loss of 20 dB.

DD FORM 1 JAN 73 1473 EDITION OF 1 NOV 65 IS OBSOLETE
S/N 0102-014-6601

251 950

CONTENTS

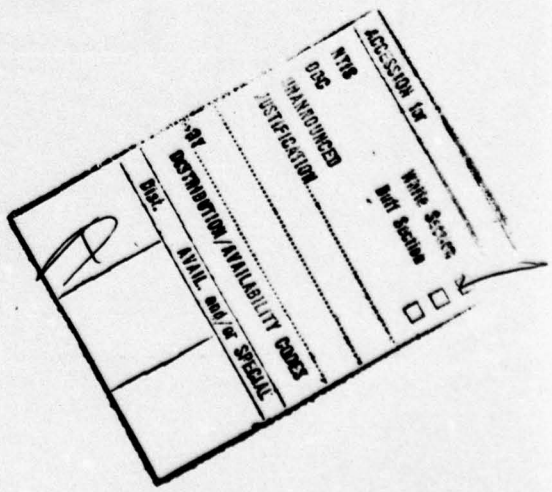

PERFORMANCE LIMITS OF A DUAL-ACOUSTIC-CHANNEL SURFACE-ACOUSTIC-WAVE (SAW) INTERFEROMETER

INTRODUCTION

As part of the joint Navy-Air Force program to develop a global satellite navigation system, NAVSTAR Global Positioning System (GPS), NRL will launch Navigation Technology Satellite One (or Timation III) in mid 1977. This satellite works in conjunction with three Air Force *navigation demonstration satellites* to demonstrate an instantaneous navigational fix capability. The work reported here was motivated by one of the problems associated with the system, namely, interference in the ground stations from the glide-path signals that aircraft use to chart their approaches into nearby airports. The portion of the UHF band allocated by the Federal Aviation Administration for the glide-path signals falls between 329.15 and 335.00 MHz; the signals themselves are separated by precisely 150 kHz.

To eliminate the glide-path interference without significantly affecting the GPS signals, Chao and Breetz developed a surface-acoustic-wave (SAW) interferometer [1]. The configuration used is indicated in Fig. 1. By combining the signals from the delay and reference arms, they achieved 13 consecutive nulls falling between the limits 49 and 65 dB. To achieve nulls of this magnitude, extremely close amplitude balance must be maintained over the frequency band of interest. The amplitude variations inherent in the SAW delay line made it essential to employ limiting amplifiers to equalize the two arms. Employing amplifiers in the saturated mode unfortunately also introduces excessive extraneous noise, seriously degrading the system sensitivity.

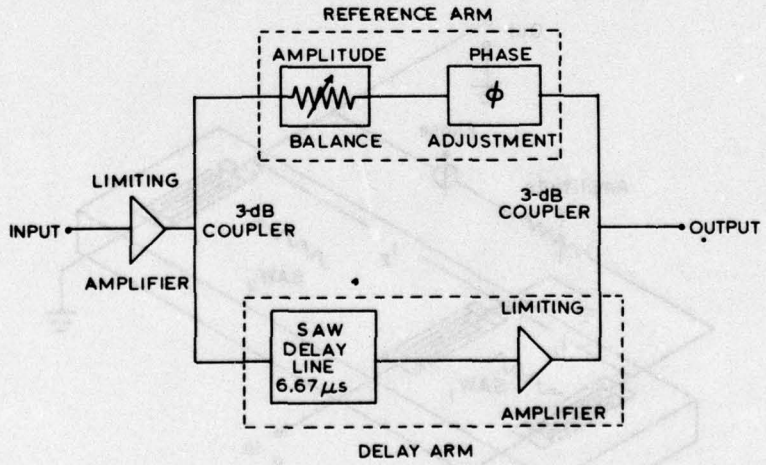

Fig. 1 — SAW interferometer using one acoustic and one electromagnetic arm (after Chao and Breetz [1])

Manuscript submitted March 8, 1977

This report evaluates another approach toward the nulling of the multiple glide-path frequencies which does not require use of the limiting amplifiers. The interferometer principle is still employed, but, rather than the electromagnetic arm and an acoustic arm shown in Fig. 1, two acoustic arms are used having a delay difference chosen to realize the desired null spacings. This report describes the design and testing of this device, evaluating the effect of numerous spurious effects on the interferometer performance. It will be shown that, with proper design, null depths approaching 50 dB can be achieved over the entire frequency band of interest (329.15 to 335.00 MHz). A single frequency within the band can of course be nulled by an arbitrary amount, limited only by the degree of phase and amplitude control provided and by stability considerations.

BASIC THEORY OF THE SAW INTERFEROMETER

Basic to all interferometers is the combining of two coherent signals which have traversed different-length delay paths. The delay difference brings about periodic interference nulls whose depths are a sensitive function of the amplitude balance between the two signals. The dual-acoustic-arm version considered in this report is shown schematically in Fig. 2. An electrical signal applied to a conventional interdigital transducer launches contra-directed surface acoustic waves as shown. An input signal of the form $Ae^{-j\omega t}$ results in signals from each of the two output transducers of the form $B_i e^{-j\omega(t-\tau_i)}$. Here t is the instantaneous time and τ_i is the delay time of SAW for $i = 1, 2$. When the amplitudes of the two channels are equalized with the variable attenuator and the phase shifter is set to a value ϕ_0, the combined output signal S from the two arms is

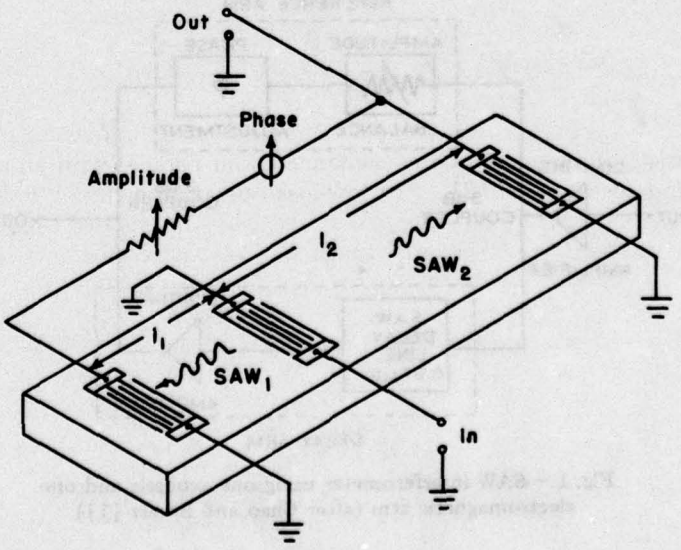

Fig. 2 — Basic dual-acoustic-arm interferometer

$$S = Be^{-j\omega t}\left[e^{-j(\omega\tau_1 + \phi_0)} + e^{-j\omega\tau_2}\right]. \tag{1}$$

After some trigonometric manipulations Eq. (1) can be written in the form

$$S = 2\,Be^{-j(\omega\tau_1 + \omega\tau_2 + \phi_0)/2}\cos\left[(\omega\tau_1 - \omega\tau_2 - \phi_0)/2\right]. \tag{2}$$

The null frequencies are determined by the condition $S = 0$. This implies

$$(\omega_n\tau_1 - \omega_n\tau_2 - \phi_0)/2 = (2n + 1)\pi/2. \tag{3}$$

When the substitutions $\omega_n = 2\pi f_n$ and $\tau_1 = \ell_i/V$ are made, where V is the SAW velocity, Eq. (3) may be rewritten as

$$\frac{fn}{V}(\ell_1 - \ell_2) = \frac{2n+1}{2} + \frac{\phi_0}{2\pi}. \tag{4}$$

The frequency spacing between adjacent nulls Δf is therefore

$$\Delta f = f_{m+1} - f_m = \frac{V}{\ell_1 - \ell_2}. \tag{5}$$

The null frequency spacing for a given SAW substrate is thus set by the transducer separations; the precise null frequencies are set by proper selection of ϕ_0.

PARAMETERS CHARACTERIZING THE SAW TRANSDUCER

A SAW interdigital transducer can be modeled by the equivalent circuit shown in Fig. 3. It consists of the electrode capacitance C_T in parallel with an acoustic radiation conductance and susceptance [2]. For low-loss operation a tuning inductor L is commonly used to resonate the capacitor at the center frequency of the band of interest. In practice parasitic capacitance arising from the transducer pads and connectors is often significant; this capacitance is denoted by C_s in Fig. 3.

The SAW transducer is conveniently characterized by means of the power scattering coefficient [3] P_{ij}:

$$P_{ij} \triangleq P_i/(P_{\text{avail}})_j, \tag{6}$$

where P_i is the power transmitted or reflected from port i and $(P_{\text{avail}})_j$ is the power available from a matched generator at port j. Since the SAW transducer is bidirectional, there are two acoustical ports, denoted by subscripts 1 and 2, and one electrical port, denoted by subscript 3. The two quantities of interest are P_{31}, which determines the insertion loss of the device, and

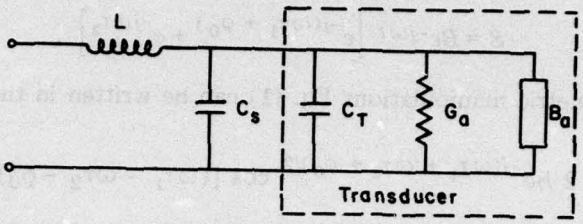

Fig. 3 — Transducer-equivalent circuit plus tuning inductor L and parasitic capacitance C_s

P_{11}, which determines the level of spurious acoustic reflected signals within the SAW delay line.

From reference 3,

$$P_{31} = \frac{2\hat{Y}_r}{(1 + \hat{Y}_r)^2 + \hat{Y}_i^2} \tag{7a}$$

and

$$P_{11} = \frac{1}{1 + 2\hat{Y}_r + |\hat{Y}|^2}, \tag{7b}$$

where $\hat{Y}$ = load on the electrical port $\div G_a$,

$\hat{Y}_r$ = real part of $\hat{Y} \div G_a$, and

$\hat{Y}_i$ = imaginary part of $\hat{Y} \div G_a$.

With the assumption that the transducer is loaded by a real impedance Z_L and with the definition $C_T + C_s \triangleq C'_T$,

$$\hat{Y} = \frac{\dfrac{1}{Z_L + j\omega L} + j\omega C'_T}{G_a}$$

$$= \frac{Z_L}{G_a(Z_L^2 + \omega^2 L^2)} + j\,\frac{\omega C'_T Z_L^2 - \omega L(1 - \omega^2 L C'_T)}{G_a(Z_L^2 + \omega^2 L^2)}$$

$$= \hat{Y}_r + j\hat{Y}_i \tag{8}$$

and

$$|\hat{Y}|^2 = \hat{Y}\hat{Y}^* = \frac{1}{G_a^2}\left[\frac{1 - 2\omega^2 LC'_T + \omega^2 C'^2_T\,(Z_L^2 + \omega^2 L^2)}{Z_L^2 + \omega^2 L^2}\right]. \tag{9}$$

After much algebra,

$$P_{11} \approx \frac{G_a^2(Z_L^2 + \omega^2 L^2)}{1 + \omega^2 C'^2_T(Z_L^2 + \omega^2 L^2) - 2\,\omega^2 C'^2_T L} \tag{10}$$

and

$$P_{31} \approx \frac{2\,Z_L G_a}{(\omega^2 LC'^2_T - 1)^2 + 2\,Z_L^2\omega^2 C'^2_T + 2\,Z_L G_a} \tag{11}$$

for $G_a \ll \omega C'_T$, a condition easily met for all transducers discussed in this report.

The conversion loss L_{31} and reflection loss L_{11} are given by the expressions

$$L_{31} = -\,10 \log P_{31} \tag{12a}$$

and

$$L_{11} = -\,10 \log P_{11}. \tag{12b}$$

For a delay line with identical input and output transducers and negligible SAW propagation loss, the insertion loss is simply $2L_{31}$. Equations (10) through (12) form the basis of the SAW interferometer design.

GENERAL CONSIDERATIONS OF SECOND-ORDER EFFECTS

To realize a series of deep nulls, as is required for the present application, the band-pass (amplitude-vs-frequency) characteristics of the two acoustical channels must be closely matched. With proper adjustment of the external amplitude and phase controls (Fig. 2), a single frequency can be nulled by an arbitrarily large amount. However in a practical device second-order effects are present which prevent a large number of deep nulls from being achieved simultaneously with a single setting of the variable attenuator and phase shifter.

The second-order effects are of two types. One type consists of spurious signals such as acoustical reflections within the delay lines and direct coupling (electromagnetic break-through) from the input transducer to the output transducers. Since these spurious signals in general have a different phase-vs-frequency and/or amplitude-vs-frequency dependance from the main signal, they cannot be simply compensated for over a band of frequencies.

The second main type of second-order effects consists of factors which prevent the primary acoustical radiated signals from tracking in amplitude precisely over the frequency band of the nulls. Within this category are transducer imperfections, diffraction, and attenuation. In the next two sections the two types of second-order effects will be treated quantitatively.

SPURIOUS-SIGNAL SECOND-ORDER EFFECTS

To determine the degree to which a spurious signal can degrade the null ratio, we will assume that in addition to the main signals from the two channels, adjusted so that both have amplitude B, there exists a signal of amplitude ηB ($\eta \ll 1$) which cannot be compensated for with the external circuitry over the entire band of interest. The null ratio N is given by the expression

$$N \triangleq -20 \log \frac{S_{\max}}{S_{\min}} \approx -20 \log \frac{2B}{\eta B} \tag{13}$$

or

$$N = 20 \log \eta - 6 \text{ dB}, \tag{14}$$

where $S_{\max}$ and $S_{\min}$ are the maximum and minimum signal amplitudes within the null frequency band. But $-20 \log \eta$ is simply the power level in dB of the spurious signal relative to one of the main signals; that is, *the null ratio is 6 dB more than the relative spurious signal level.*

When M spurious signals are present, the worst-case null ratio will be

$$N = 20 \log \sum_{i=1}^{M} \eta_i - 6 \text{ dB}. \tag{15}$$

In practice the external phase shifter and attenuator are adjusted slightly to attempt to avoid this condition, often with the null frequency being shifted by a finite but tolerable amount.

From Eq. (14) it is evident that, to achieve 50-dB nulls with a single spurious signal present, the spurious signal must be 44 dB below the main signal. If a second spurious signal is present, 6 dB smaller than the first ($\eta_2 = 0.5\eta_1$), then

$$\begin{aligned} N(\eta_1, \eta_2) &= 20 \log (\eta_1 + 0.5\eta_1) \text{ dB} \\ &= N(\eta_1) + 3.5 \text{ dB}. \end{aligned} \tag{16}$$

In this case the two spurious levels must be 46.5 dB and 52.5 dB respectively below the main signal to be certain of achieving a 50-dB null ratio.

A prominant spurious signal is electromagnetic leakage, namely, energy which couples directly from the input of the delay line to the output without being converted to acoustical energy. In general the phase variation across any reasonably small fractional bandwidth (as in the present case) will be negligible. However, since amplitude variations of ≈1 dB are common, a single setting of the attenuator and phase shifter cannot compensate for this spurious signal. Nevertheless, with careful design and packaging, leakage will not be the controlling factor in determining the null depth. Care must be taken to ground all nonsignal-carrying metal and to isolate all tuning inductors to minimize direct crosstalk. It is also common to place grounded metal strips on the SAW substrate between transducers for additional suppression.

Another significant spurious signal in the SAW interferometer arises from acoustical reflections from the transducers. The *triple-transit* signal is an example in this category. The triple-transit signal appears at the output, delayed from the main signal by twice the SAW propagation time. Physically it arises from successive acoustical reflections from the output and input transducers before being coupled to the receiver. Because it has transversed three times the acoustical path length of the main signal, it posses a significantly different phase-frequency response.

The reflected wave cannot be completely eliminated, since a conventional transducer is a three-port device and it is a general property of such devices that all ports cannot be simultaneously matched. A tradeoff is necessary between low conversion loss (L_{31}) and low acoustical reflection (L_{11}). For the equivalent circuit of Fig. 3 the tradeoff can be computed from Eqs. (10) through (12). This is shown in Fig. 4 for a transducer design appropriate for the present application. The tuning inductor L is used as a variable parameter.

For this example, to achieve 50-dB nulls when a single triple-transit echo dominates the spurious response, the conversion loss of that channel can be no less than 10 dB (Eq. (14)).

The type of acoustical reflections discussed thus far are *regenerative*; that is, they result from electrical energy being reflected from the transducer terminations and regenerating acoustical signals. A second source of reflection occurs because of the physical presence of the periodic metallic transducer pattern on the surface of the acoustic medium. An acoustic wave traveling under a metallic stripe exhibits a different velocity and wave impedance than it exhibits on the free surface. The change occurs because the metallic-mass loading alters the effective elastic properties of the medium and because the electric field which accompanies the wave (due to the piezoelectric properties of the crystal) is shorted out at the surface. The shorting alters the interaction between the wave, its traveling field, and the crystal.

The impedance changes encountered by the wave in passing from a metallized to a nonmetallized region (or vice versa) cause a portion of the incident wave to be reflected. In a conventional interdigital transducer (quarter-wave electrodes separated by quarter-wave

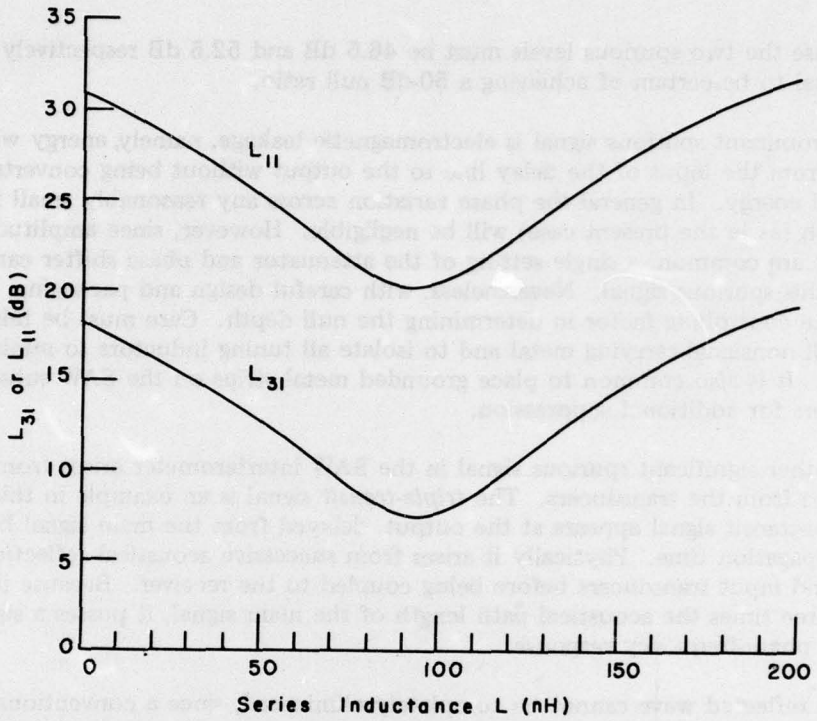

Fig. 4 — Tradeoff between insertion loss and regenerative reflection loss for a SAW transducer. The transducer parameters are R_a (= $G_a\omega^2 C_T^2$) = 15Ω, C_T = 1.5 *pF*, C_S = 1.0 *pF*, and F = 330 MHz.

spaces), the reflections will add in phase with each other and also with the regenerated wave at the synchronous transducer frequency (as given by L_{11}). The fractional impedance change $\Delta Z/Z$ has been shown to be [4]

$$\frac{\Delta Z}{Z} = \frac{2}{3}\,\frac{m_{\text{metal}}}{m_{\text{substrate}}}\,\frac{h}{\lambda} + \frac{1}{2}\,k^2, \tag{16}$$

where m_{metal} and $m_{\text{substrate}}$ are the mass densities of the metal and substrate respectively, h is the metal thickness, λ is the acoustic wavelength, and k^2 is the electromechanical coupling constant.

For n discontinuities (n/2 electrodes), the reflection coefficient Γ for a transducer is given by [5]

$$\frac{1+\Gamma}{1-\Gamma} = \left(1 + \frac{\Delta Z}{Z}\right)^n. \tag{17}$$

The mechanical and electrical discontinuities thus result in a reflected wave which is

$$L_{11}' = -20 \log \Gamma \text{ dB} \tag{18}$$

below the incident wave.

For weak-coupling-constant materials such as quartz ($k^2 \approx 0.002$) the field-shorting term can be neglected. Obviously the mechanical discontinuity can be reduced by reducing the metal thickness h. There is a practical lower limit to this reduction, however, since the finger resistance increases with decreasing h, thus increasing L_{31}. Quantitatively the finger resistance R_s is given by [6]

$$R_s = \frac{8}{3} \rho_s \frac{\hat{W}}{N} \tag{19}$$

where ρ_s is the metal surface resistivity, N is the number of transducer finger pairs, and $\hat{W}$ is the transducer aperture in acoustical wavelengths.

We have calculated the dependence of insertion loss on film thickness by using typical ρ_s versus h values [7] to determine R_s and inserting R_s in a series with L in Fig. 3. The conversion loss can then be straightforwardly calculated in the manner used to derive Eqs. (10) and (11). Figure 5 shows the dependence of L_{31} and L_{11} on metal

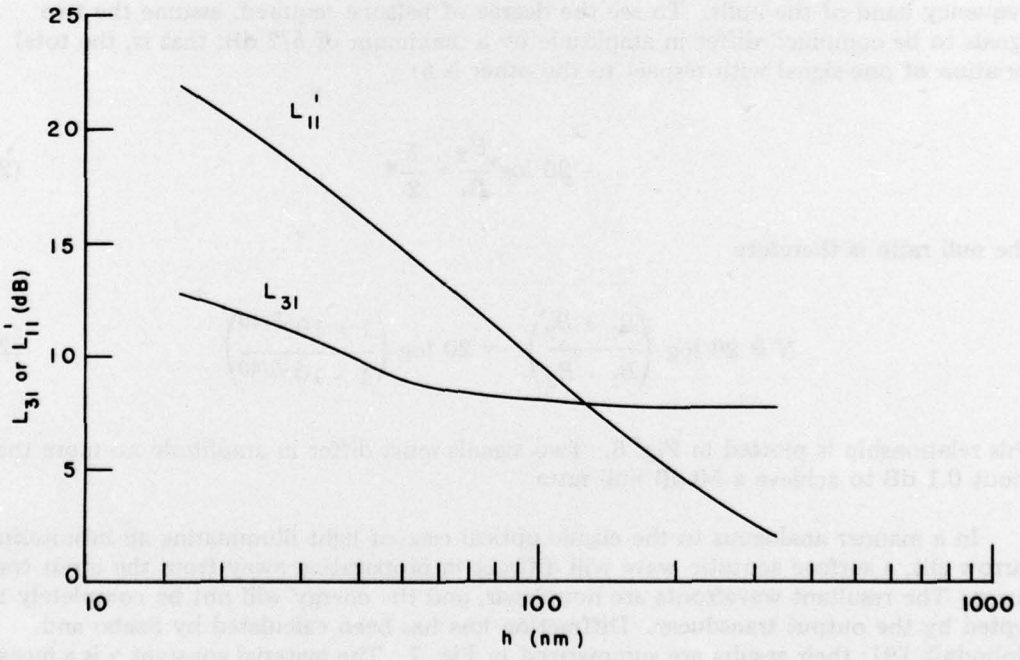

Fig. 5 — Tradeoff between insertion loss and mechanical mismatch reflection loss for a SAW transducer. The transducer parameters are $R_a = 15\Omega$, $C_T = 1.5\ pF$, $C_S = 1.0\ pF$, $L = 92$ nH, and $f =$ MHz.

(aluminum) film thickness for the same set of transducer parameters as given in Fig. 4. L is adjusted to resonate the total capacitance at the transducer synchronous frequency. To achieve 50-dB nulls, the aluminum thickness cannot exceed 20 nm. A film this thin results in ohmic losses of about 5 dB, making the single-channel insertion loss nearly 25 dB.

The discussion has assumed a transducer with quarter-wavelength fingers and spaces. As was noted, individual reflections due to electrical and mechanical discontinuities will add in phase at the transducer synchronous frequency. By use of a *double-electrode* configuration [8], (electrodes and spaces 1/8 wavelength wide) this source of reflection can be significantly reduced. A disadvantage of this configuration is that the transducer fingers are half as wide as those of a standard transducer, and the fabrication procedure may be considerably complicated. However efficient operation at the third harmonic frequency of the double-electrode transducer is possible in many cases [8], alleviating this difficulty.

Another source of spurious signals is bulk-wave generation and detection by the interdigital transducer. Although these signals may have sufficient amplitude to be troublesome, they will occur only out of the frequency range of interest for the present application.

CHANNEL-AMPLITUDE-IMBALANCE SECOND-ORDER EFFECTS

As was noted, the amplitudes of the two channels must track precisely over the frequency band of the nulls. To see the degree of balance required, assume the two signals to be combined differ in amplitude by a maximum of $\delta/2$ dB; that is, the total variation of one signal with respect to the other is δ:

$$-20 \log \frac{B_2}{B_1} = \frac{\delta}{2}. \tag{20}$$

The null ratio is therefore

$$N \triangleq 20 \log \left(\frac{B_1 + B_2}{B_1 - B_2} \right) = 20 \log \left(\frac{1 + 10^{-\delta/40}}{1 - 10^{-\delta/40}} \right) \tag{21}$$

This relationship is plotted in Fig. 6. Two signals must differ in amplitude no more than about 0.1 dB to achieve a 50-dB null ratio.

In a manner analogous to the classic optical case of light illuminating an infinitesimally narrow slit, a surface acoustic wave will diffract in propagating away from the input transducer. The resultant wavefronts are nonplanar, and the energy will not be completely intercepted by the output transducer. Diffraction loss has been calculated by Szabo and Slobodnik [9]; their results are summarized in Fig. 7. The material constant γ is a measure of velocity anisotropy and has been cataloged for the most commonly used SAW materials

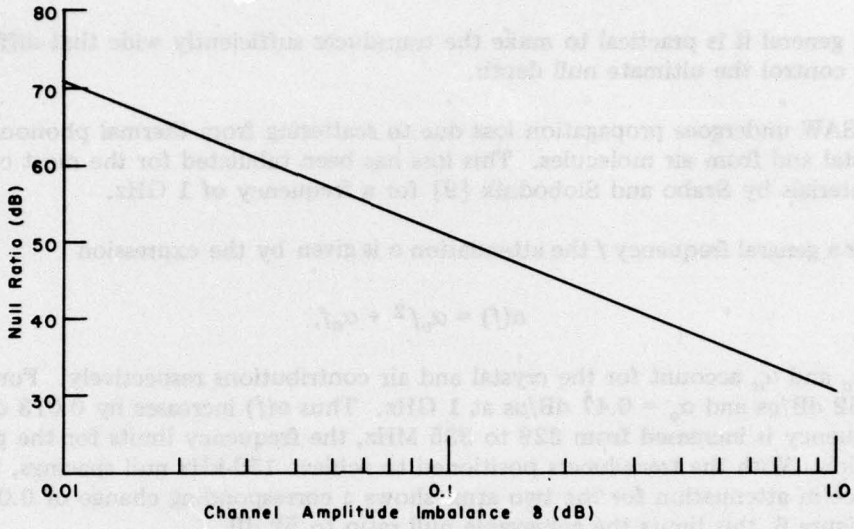

Fig. 6 — Null ratio of an interferometer as a function of a difference in amplitude between the two channels

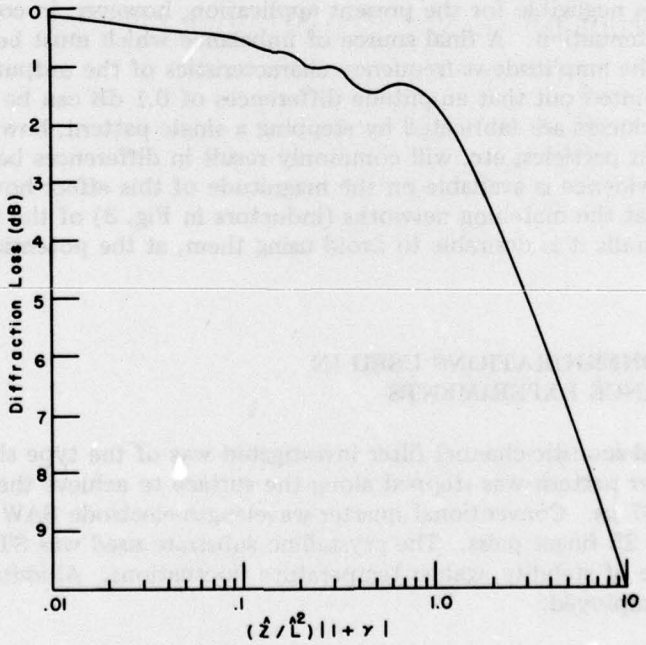

Fig. 7 — Diffraction loss of a surface-acoustic-wave delay line of transducer aperture $\hat{Z}$ and transducer separation $\hat{L}$. The abscissa units are in acoustical wavelengths, with γ being a material parameter [9].

[9]. In general it is practical to make the transducer sufficiently wide that diffraction will not control the ultimate null depth.

A SAW undergoes propagation loss due to scattering from thermal phonons within the crystal and from air molecules. This loss has been tabulated for the most commonly used materials by Szabo and Slobodnik [9] for a frequency of 1 GHz.

For a general frequency f the attenuation α is given by the expression

$$\alpha(f) = \alpha_v f^2 + \alpha_a f, \tag{22}$$

where α_v and α_a account for the crystal and air contributions respectively. For quartz α_v = 2.62 dB/μs and α_a = 0.47 dB/μs at 1 GHz. Thus $\alpha(f)$ increases by 0.013 dB/μs as the frequency is increased from 329 to 335 MHz, the frequency limits for the present application. With the transducers positioned to achieve 150-kHz null spacings, the total difference in attenuation for the two arms shows a corresponding change of 0.09 dB. From Figure 6, this limits the achievable null ratio to 52 dB.

Another source of channel amplitude imbalance is beam steering, that is, failure of a SAW to transverse a straight-line path from input to output because of crystalline anisotropy [9]. This is negligible for the present application, however, in comparison to diffraction and attenuation. A final source of imbalance which must be considered is the degree to which the amplitude-vs-frequency characteristics of the output transducers match. It was pointed out that amplitude differences of 0.1 dB can be significant. In practice the transducers are fabricated by stepping a single pattern; however any crystal imperfections, dust particles, etc. will commonly result in differences between the two. No quantitative evidence is available on the magnitude of this effect however. One also must take care that the matching networks (inductors in Fig. 3) of the two transducers track. For deep nulls it is desirable to avoid using them, at the potential sacrifice of some insertion loss.

DELAY-LINE CONFIGURATIONS USED IN PERFORMANCE EXPERIMENTS

The first dual-acoustic-channel filter investigated was of the type shown in Fig. 2. A single transducer pattern was stepped along the surface to achieve the required delay differential of 6.67 μs. Conventional quarter-wavelength-electrode SAW transducers were employed, having 25 finger pairs. The crystalline substrate used was ST-quartz, chosen for its high degree of stability against temperature fluctuations. Aluminum transducer electrodes were employed.

This approach was eventually abandoned because of excessively high spurious signal levels. The reflection of SAW_1 (Fig. 2) from its output transducer will appear at the output transducer of SAW_2 at a power level of only L_{11} + 2 times the propagation loss of path ℓ_1 below the level of SAW_2. This single-bounce-echo level was measured to be less than 20 dB below the primary signal, clearly unacceptable for achieving deep nulls.

To alleviate the problem, the configuration shown in Fig. 8 was employed. Since the output transducers are no longer collinear, an acoustical reflection from one output transducer must be converted at the center transducer to an electrical signal and then reconverted to an acoustical signal to be transmitted to the other output transducer. The single-bounce echos are thus $2L_{31}$ (where L_{31} is the conversion loss of the center transducers), smaller than the single-bounce echo of the Fig. 2 configuration.

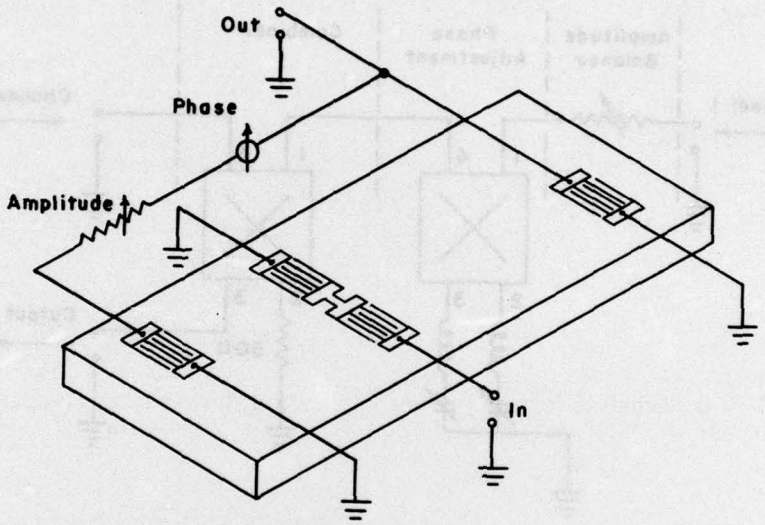

Fig. 8 — Dual-acoustic-arm SAW interferometer using offset acoustic channels

The disadvantage of the new configuration is that each of the individual center transducers is now electrically loaded by the other. Values of L_{11} and L_{31} for the double-center-transducer offset-channel configuration can be derived by a straightforward extension of the scattering-parameter development of Eqs. (6) through (12) for the single-center-transducer collinear-channel configuration. For the transducer parameters shown in Fig. 4 (and also used in our experiments) an increase of L_{31} by 1 dB and L_{11} by 4 dB at resonance were calculated for the two-series-transducer arrangement. In general, since weak coupling is essential to keep the regenerated triple-transit signal small, the conversion loss of the offset-channel configuration (Fig. 8) is not significantly more than that of the collinear-channel configuration (Fig. 1), and the offset-channel configuration exhibits much lower spurious acoustical echo levels.

We chose not to undergo the added complexity of the double-electrode configuration but to use standard quarter-wave finger and gap transducers. Thus it was essential to use thin metalic fingers to minimize mechanical reflections. The final devices employed 50 nm of aluminum.

EXTERNAL CIRCUITRY

Three functions must be performed by the circuitry external to the SAW delay line shown in Fig. 8: attenuation of the largest amplitude signal of the two channels, phase shifting to set the nulls at the desired frequencies, and efficient combination of the two signals. Independent control of amplitude and phase are highly desirable.

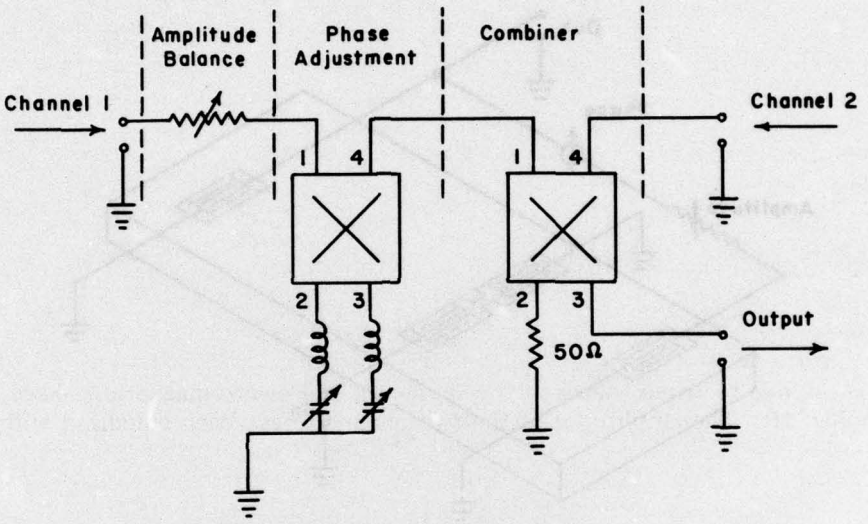

Fig. 9 — Network for combining the two channels and adjusting the null frequency and depth

The basic circuitry we employed is shown in Fig. 9. Quadrature hybrids were used for both the phase shifter and combiner. Ideally a signal applied to port 1 (or port 4) of the hybrid will split equally between ports 2 and 3, the output at the latter ports differing in phase by 90°. For a signal applied to port 2 (or port 3) the roles of 1 and 4 and 2 and 3 are interchanged.

Thus in the phase-shifter section a signal applied to port 1 will appear unattenuated from port 4 because of the equal reactive loads at ports 2 and 3. However the phase of the signal at port 4 can be adjusted by the setting of the variable capacitors. The quadrature-hybrid combining approach used here is very efficient in comparison to simple tee or coupler combiners, since signals which are 90° out of phase at ports 1 and 4 will be 100% transferred to either port 3 or port 2.

The ideal operation just described can be approached only if ports 2 and 3 as well as ports 1 and 4 are terminated with the same impedance. The terminations for the two sets are of course not necessarily equal. Since the transducer impedance is approximately 15 Ω and a variable resistance is necessary to balance the channel amplitudes, the equal-impedance condition cannot be met exactly. Since the loss to the long acoustic arm exceeded that in the short arm by 4 to 5 dB by virtue of added diffraction and propagation

attenuation, loss per se due to mismatch in the phase-adjustment and combining networks was not a problem. What did prove troublesome was the interaction between frequency shifting (phase shifting) and null-depth adjustment (amplitude control); that is, slight frequency adjustments would change the null depth, and vice versa. Various resistive-capacitive combinations were investigated, such as parallel RC combinations to simulate the transducer impedances, but the relatively simple form shown in Fig. 9 proved most effective in separating the two functions.

The actual circuitry fabricated employed stripline quadrature hybrids (Merrimac model QHF-2-.312G). Variable capacitors, tunable from 4 to 40 *pF*, were adequate to set the desired frequency. A low-inductance variable resistor of 0 to 500 ohms was used to balance the amplitudes. The surface-wave substrate itself was packaged in a flat pack. The entire interferometer, including external circuitry, fit easily within a 6-by-10-by-4-cm standard (Pomona) aluminum box.

EXPERIMENTAL PERFORMANCE

The interferometer was first evaluated using standard pulse-echo techniques to ascertain the spurious signal level. Relative levels of the most prominent spurious signals, namely, those due to triple transit in the short arm and electromagnetic leakage, are shown in Fig. 10. The amplitudes of the two channels have been equalized with the variable attenuator. Half the power of each signal is dissipated in the load at the combiner-hybrid (port 2). Slight errors in the transducer fabrication caused the bandpass center to be skewed to the high end of the desired range of the nulls, resulting in a loss differential

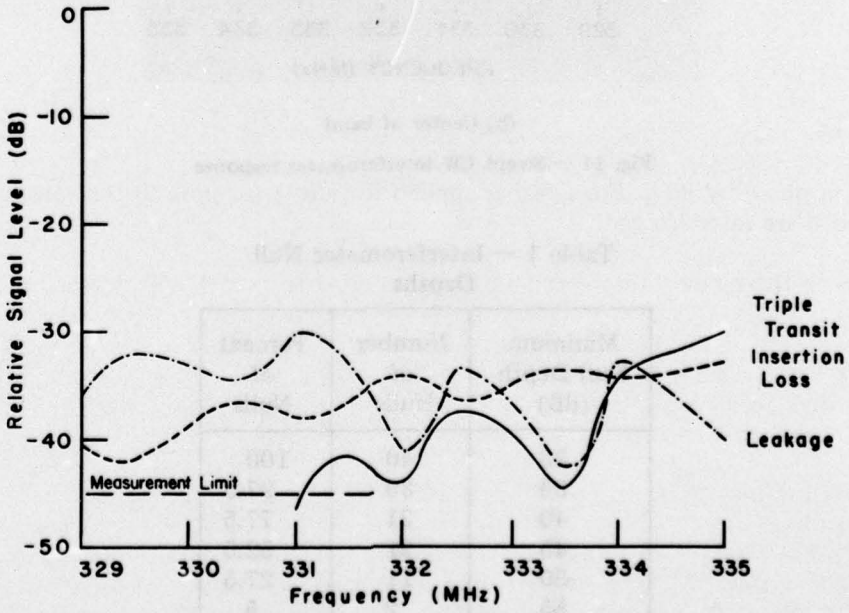

Fig. 10 — Pulse-echo measurements of the electromagnetic-leakage signal, the triple-transit signal, and the insertion loss

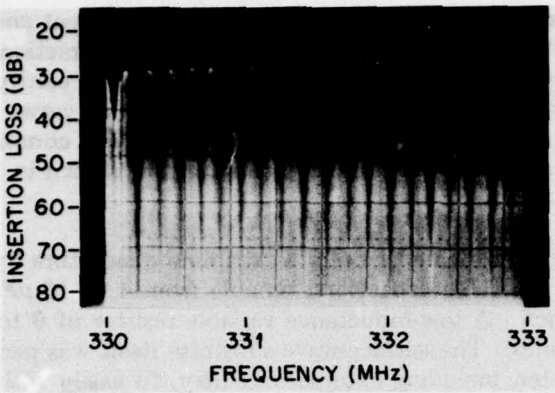

(a) Entire band

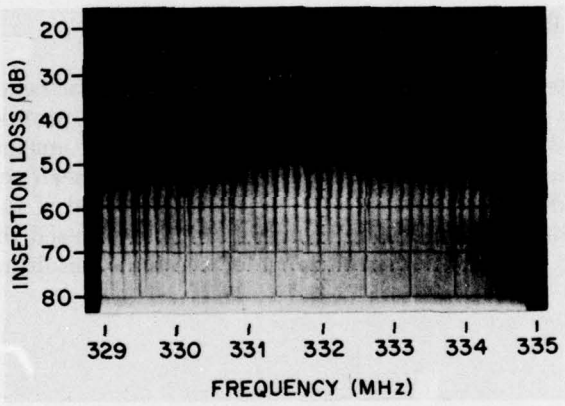

(b) Center of band

Fig. 11 — Swept CW interferometer response

Table 1 — Interferometer Null Depths

Minimum Null Depth (dB)	Number of Nulls	Percent of Nulls
33	40	100
35	39	97.5
40	31	77.5
45	21	52.5
50	11	27.5
55	2	5

of 7 dB from one band edge to the other. The triple-transit signal is the dominant spurious signal at the tupper end of the band, and electromagnetic leakage dominates at the lower end.

A photograph of the nulls over the entire 329-to-335-MHz frequency band of interest is shown in Fig. 11a, and a photograph over the center portion of the band is shown in Fig. 11b. The minimum insertion loss is 6 dB less than the individual losses in the pulse-echo measurements because of the coherent addition of the signals from the two arms. The nulls in these figures appear somewhat deeper than they are. A summary of point-by-point CW measurements is shown in Fig. 12 and cataloged in Table 1. The poorest of the 40 null depths is 33 dB; however more than half of the nulls are 45 dB or better.

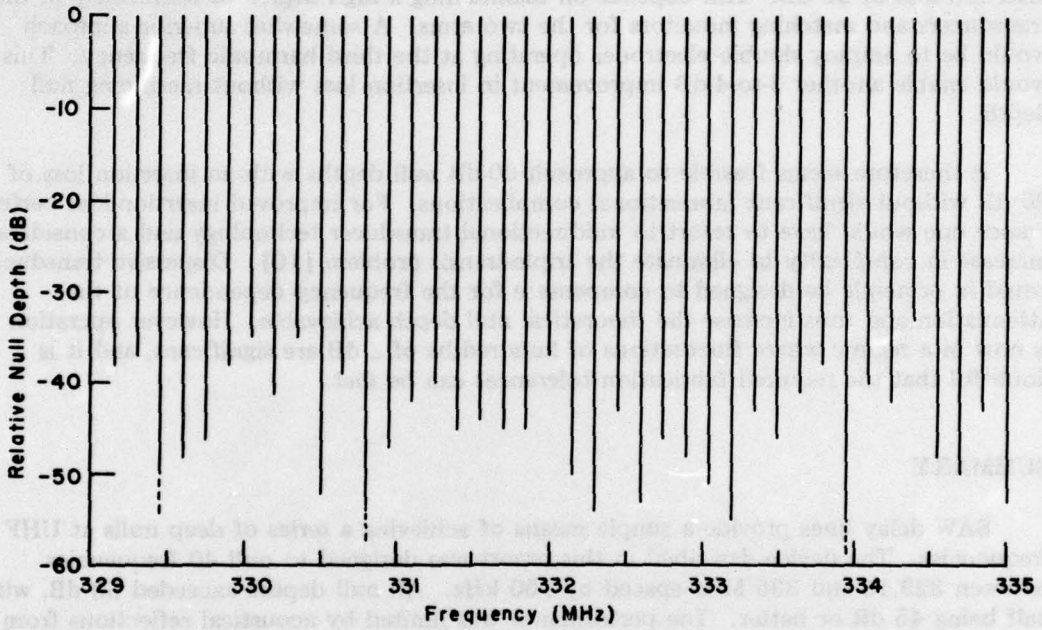

Fig. 12 — CW null depths

DISCUSSION

The null depth obtained in the experimental prototype are considerably less than the diffraction and attenuation limits discussed with reference to Figs. 4 through 7. From the previous section it is evident that the most serious spurious signal is the triple-transit signal from the short acoustical path, although the leakage is also somewhat troublesome. From Figs. 4 and 5 it is further evident that for the 50-nm-thick aluminum transducer pattern used, mechanical and not regenerative reflections are predominant. In fact the measured 30-dB triple-transit suppression ($2L_{11}$) is in reasonable agreement with the predicted level for mechanical reflections.

The pulse-echo insertion loss of 33 dB for the long path and 29 dB for the short path (including external circuitry) was significantly higher than the calculated value, although the attenuation difference between the two paths is consistent with propagation-loss and diffraction-loss calculations. The insertion loss of the prepackaged SAW delay lines was 6 to 7 dB less than these results. The deterioration is probably due to the deposition of foreign matter on the delay lines which could not be completely removed. The calculated minimum insertion loss was 20 dB; thus parasitic capacitance and/or resistance were seemingly slightly higher than anticipated.

Using the present design and reducing the aluminum thickness to less than 20 nm, is should be theoretically possible to approach null depths of 50 dB with a minimum insertion loss of 25 dB. This depends on maintaining a high degree of uniformity in the transducers and matching inductors for the two arms. A somewhat superior approach would be to employ double electrodes operating at the third harmonic frequency. This would enable another 3-to-4-dB improvement in insertion loss without sacrificing null depth.

It therefore seems feasible to approach 50-dB null depths with an insertion loss of 20 dB without significant fabricational complications. For improved insertion-loss performance one would have to resort to unidirectional transducer technology and a considerable increase in complexity to eliminate the triple-transit problem [10]. Dispersive transducers could in principle be designed to compensate for the frequency dependence of the attenuation and thus increase the theoretical null depth achievable. However operation is now in a regime where fluctuations of hundredths of a dB are significant, and it is doubtful that the required fabrication tolerances can be met.

SUMMARY

SAW delay lines provide a simple means of achieving a series of deep nulls at UHF frequencies. The device described in this report was designed to null 40 frequencies between 329.15 and 335 MHz spaced by 150 kHz. All null depths exceeded 33 dB, with half being 45 dB or better. The performance was limited by acoustical reflections from the transducers. Analysis of second-order effects showed that 50-dB nulls over the band of interest are feasible with an attendant insertion loss of 20 dB. By using stripline quadrature hybrids for phase shifting and combining networks, and ST-quartz for the SAW substrate, a highly compact, temperature-stable, high-performance device can be realized.

REFERENCES

1. G. Chao and L. Breetz, "Surface Acoustic Wave UHF Interferometer," IEEE Trans. Microwave Theory Tech. MTT-22, 908-910 (Oct. 1974).

2. W.R. Smith, H.M. Gerard, J.H. Collins, T.M. Reeder, and H.J. Shaw, "Analysis of Interdigital Surface Wave Transducers by Use of an Equivalent Circuit Model," IEEE Trans. Microwave Theory Tech. MTT-17, 856-864 (Nov. 1969).

3. H.M. Gerard, "Acoustic Scattering Parameters of the Electrically Loaded Interdigital Surface Wave Transducer," IEEE Trans. Microwave Theory Tech. MTT-17, 1045-1046 (Nov. 1969).

4. W.R. Smith, "Basics of the SAW Interdigital Transducer," Wave Electronics 2, 25-63 (July 1976).

5. E.K. Sittig and G.A. Coquin, "Filters and Dispersive Delay Lines Using Repetitively Mismatched Ultrasonic Transmission Lines," IEEE Trans. Sonics and Ultrasonics SU-15, 111-119 (Apr. 1968).

6. K.M. Lakin, "Electrode Resistance Effects in Interdigital Transducers," IEEE Trans. on Micro. Theory and Tech. MTT-22, 418-424 (Apr. 1974).

7. R.C. Rosenfield and C.S. Hartman, "Subminiature Broadband Filters," Interim Technical Report, contract DAAB07-72-C-0326, Texas Instruments, Inc., Dallas, Tex., Feb. 1973.

8. T.W. Bristol, W.R. Jones, P.B. Snow, and W.R. Smith, "Applications of Double Electrodes in Acoustic Surface Wave Device Design," 1972 Ultrasonics Symposium Proceedings, IEEE catalog number 72 CHO 708-8 SU, pp. 343-345, Oct. 1972.

9. T.L. Szabo and A.J. Slobodnik, Jr., "The Effect of Diffraction on the Design of Acoustic Surface Wave Devices," IEEE Trans. Sonics and Ultrasonics SU-20, 240-251 (July 1973).

10. C.S. Hartmann, W.S. Jones, and H. Vollers, "Wideband Unidirectional Interdigital Surface Wave Transducers," IEEE Trans. Sonics and Ultrasonics SU-19, 378-381 (July 1972).